Provided for non-commercial research and education use.
Not for reproduction, distribution or commercial use.

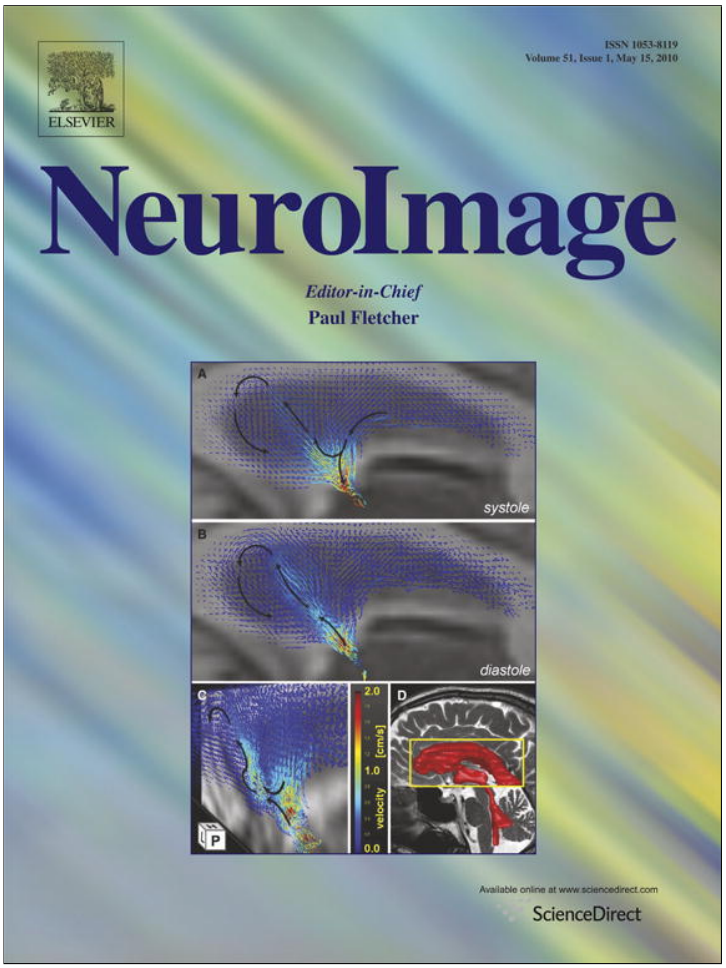

This article appeared in a journal published by Elsevier. The attached copy is furnished to the author for internal non-commercial research and education use, including for instruction at the authors institution and sharing with colleagues.

Other uses, including reproduction and distribution, or selling or licensing copies, or posting to personal, institutional or third party websites are prohibited.

In most cases authors are permitted to post their version of the article (e.g. in Word or Tex form) to their personal website or institutional repository. Authors requiring further information regarding Elsevier's archiving and manuscript policies are encouraged to visit:

http://www.elsevier.com/copyright

Author's personal copy

NeuroImage 51 (2010) 83–90

Contents lists available at ScienceDirect

NeuroImage

journal homepage: www.elsevier.com/locate/ynimg

Complexity analysis of source activity underlying the neuromagnetic somatosensory steady-state response

Vasily A. Vakorin [a,*], Bernhard Ross [a,f], Olga Krakovska [c], Timothy Bardouille [a], Douglas Cheyne [d,e], Anthony R. McIntosh [a,b]

[a] Rotman Research Institute of Baycrest, Canada
[b] Department of Psychology, University of Toronto, Canada
[c] Department of Chemistry, York University, Canada
[d] Toronto Hospital for Sick Children Research Institute, Canada
[e] Department of Medical Imaging, University of Toronto, Canada
[f] Department of Medical Biophysics, University of Toronto, Canada

ARTICLE INFO

Article history:
Received 4 June 2009
Revised 22 October 2009
Accepted 27 January 2010
Available online 2 February 2010

Keywords:
Complexity
Synchrony
Synchronization
Sample entropy
Cross-sample entropy
Steady-state response
MEG

ABSTRACT

Using the notion of complexity and synchrony, this study presents a data-driven pipeline of nonlinear analysis of neuromagnetic sources reconstructed from human magnetoencephalographic (MEG) data collected in reaction to vibrostimulation of the right index finger. The dynamics of MEG source activity was reconstructed with synthetic aperture magnetometry (SAM) beam-forming technique. Considering brain as a complex system, we applied complexity-based tools to identify brain areas with dynamic patterns that remain regular across repeated stimulus presentations, and to characterize their synchronized behavior. Volumetric maps of brain activation were calculated using sample entropy as a measure of signal complexity. The complexity analysis identified activity in the primary somatosensory (SI) area contralateral to stimuli and bilaterally in the posterior parietal cortex (PPC) as regions with decreased complexity, consistently expressed in a group of subjects. Seeding an activated source with low complexity in the SI area, cross-sample entropy was used to generate synchrony maps. Cross-sample entropy analysis confirmed the synchronized dynamics of neuromagnetic activity between areas SI and PPC, robustly expressed across subjects. Our results extend the understanding of synchronization between co-activated brain regions, focusing on temporal coordination between events in terms of synchronized multidimensional signal patterns.

© 2010 Elsevier Inc. All rights reserved.

Introduction

Characterizing functionally specific brain regions and describing their functional integration are two complimentary, not mutually exclusive, issues studied in neuroscience. One possible paradigm to tackle these issues is to consider the brain as a complex system (Jirsa and McIntosh, 2007). This approach focuses on complexity, a broadly defined property characterizing a highly variable system with many parts whose behaviors strongly depend on the behavior of other parts (Deisboeck and Kresh, 2006). Information-theoretic tools provide many ways to estimate complexity of brain signals. In general, a complex system can be characterized by its entropy, which can be related to uncertainty contained in signals. Typically, higher entropy is associated with disorder, uncertainty and unpredictability, whereas lower entropy is related to a high degree of organization. Traditional methods for estimating entropy can lose much information related to temporal properties of the signal. Based on nonlinear dynamics, a number of techniques for signal analysis have been recently designed to yield more details on inherent dynamic properties of brain activity (Stam, 2005).

Pincus (1991) developed a measure of signal regularity closely related to the Kolmogorov entropy (Grassberger and Procaccia, 1983), interpreted as an averaged rate of information produced by a dynamic system. Called approximate entropy, this statistic can be applied for short and noisy time series. Approximate entropy searches for epochs that are similar in one multidimensional representation of the original signal, and will remain similar in a space with increased dimensionality. In an attempt to reduce the bias in estimating the approximate entropy due to calculating self-matches in the signal patterns, Richman and Moorman (2000) proposed the sample entropy statistic. Similar to sample entropy in design and concept, cross-sample entropy as a refined version of cross approximate entropy was introduced as a measure of synchrony between bivariate time series (Richman and Moorman, 2000). Cross-sample entropy was designed to compare epochs from

* Corresponding author.
E-mail address: vasenka@gmail.com (V.A. Vakorin).

1053-8119/$ – see front matter © 2010 Elsevier Inc. All rights reserved.
doi:10.1016/j.neuroimage.2010.01.100

Author's personal copy

one signal with those of the second, identifying the averaged degree of similarity between them.

Recent complexity-based studies have proven useful in characterizing pathological states of brain activity such as in epilepsy and psychiatric disorders or brain dementia. Applying approximate entropy analysis to the different epochs of epileptic seizure time series, Radhakrishnan and Gangadhar (1998) observed increased complexity values at the beginning and the end of the seizure. Approximate entropy was also used to characterize the depth of anaesthetic effect using electroencephalography (EEG) recordings (Bruhn et al., 2000). A number of studies applied complexity-based tools to examine brain activity in patients with Alzheimer's disease (AD) (Hornero et al. (2009) for a review). In particular, Absolo et al. (2005) found decreased irregularity of EEG rhythms in AD patients, compared to control subjects. Similar to EEG, magnetoencephalography (MEG) activity was reported to be less complex and more regular in AD patients than in control subjects (Gmez et al., 2009). In addition, in normal brain, a comparative analysis of EEG data in five age groups, using multi-scale entropy based on sample entropy (Costa et al., 2002), indicated that brain variability increases with maturation, reflecting a broader repertoire of metastable brain states and more rapid transitions among them (McIntosh et al., 2008).

The common feature of the aforementioned studies is that they differentiate brain activity in different states based on EEG/MEG scalp measurements that do not directly represent localized brain regions in the vicinity of one electrode. Due to volume conduction, the measured potentials reflect a summed signal from simultaneously active, underlying current sources when signals of the sources become filtered and spread out across all the electrodes (Nunez and Shrinivasan, 2005). The translation to source space would be a logical extension, particularly with the recent refinements in source-space projections through the beam-former solutions. This study shows that sample entropy and cross-sample entropy statistics can be sensitive enough to work at the level of individual regions and discriminate the dynamics of neuromagnetic activity between different sources.

This study illustrates the possibility to characterize brain activity and interactions between sources using the concept of complexity with application to the somatosensory steady-state response (SSSR) evoked by a periodic tactile signal. Oscillatory steady-state response is a phenomenon observed as a reaction to applying trains of periodically repeated stimuli, in contrast to temporal patterns of transient signal changes caused by the onsets of stimulus trains (Nangini et al., 2006). Typically the SSSR, which is observed at the frequency of the driving stimulus, is smaller than the transient response, reaching its maximal amplitudes between 21 and 26 Hz (Snyder, 1992). It was suggested that the pattern of synchronization between neuronal groups dynamically determines the pattern of neuronal interactions (Womelsdorf et al., 2007). Following the idea of functional connectivity modulated by synchronous oscillations, Bardouille and Ross (2008) applied a statistic measure called intertrial coherence (ITC) (Stapells et al., 1987). In an attempt to find brain areas with the SSSR with consistent phase relations to the stimulus, they measured the degree of phase-locking inherent in a given signal. Various sensorimotor areas were identified in individual source ITC maps, but only the primary somatosensory area (SI) contralateral to stimuli was consistently identified across subjects.

ITC is calculated in the space spanned by the real component of the signal and the imaginary part reconstructed from the original signal. In essence, ITC is based on a two-dimensional reconstruction of the dynamical system underlying the observed signal. Nonlinear techniques based on multidimensional reconstruction of the dynamics of brain activity through time delay embedding might be viewed as the platform to provide a generalization of the two-dimensional complex space. The goal would be to find brain areas that are co-activated with the SSSR having consistent regular patterns. Characterizing the involved brain regions and their interaction within a wide range network would contribute to understanding the principles underlying somatosensory perception. In this study, we identified the loci of somatosensory activation, using sample entropy as a measure of complexity (regularity), and subsequently explored synchrony in the activation network, performing the cross-sample entropy analysis.

Materials and methods

Experiment

MEG data were collected at a sample rate of 1250 Hz with a bandwidth of 0–300 Hz using a 151-channel whole-head first-order gradiometer system (VSM Medtech, Port Coquitlam, BC, Canada). Subjects were seated upright with their head resting in the helmed shaped scanner. Head localization coils were placed on the nasion, and left and right pre-auricular points for co-registration of MEG data with anatomical MR images. A small elastic air bladder was fitted to the right index finger pad. Vibrotactile stimulation was applied to the finger by pressurizing the bladder with 23 Hz trains of 10 ms compressed air pulses of 3 s in duration. The inter-train interval was randomly distributed between 3 and 5 s. A white noise masking sound was binaurally presented at 90 dB SPL via insert phones to mask sounds possibly associated with the stimulator. MEG data and the driving signal for the stimulator were collected simultaneously for 10 min. Subjects watched a subtitled silent movie and were asked to stay alert during the MEG recording. No stimulus related task was required. More details on the data acquisition can be found in the study of Bardouille and Ross (2008).

Complexity: sample entropy

Many complex biophysiological phenomena are due to nonlinear effects. Recently there has been an increasing interest in studying complex neural networks in the brain, specifically applying concepts and time series analysis techniques derived from nonlinear dynamics (see Stam (2005) for a comprehensive review on nonlinear dynamical analysis of EEG/MEG). One approach to nonlinear analysis consists of reconstructing the underlying dynamical systems underlying EEG or MEG time series. Reconstruction of multivariate dynamics can be performed through the procedure called time delay embedding, in which the underlying process is represented by the same versions of the original signal shifted in time. Thus, the underlying dynamics are associated with a sequence of points in a multidimensional space with the coordinates obtained by taking the amplitude values of the original time series at several consecutive times, separated by a time lag (usually measured in data points).

Approximate entropy (Apen) was proposed to quantify the complexity of signals (Pincus, 1991, 1995). Under this account, time series are treated as samples derived from observing the underlying dynamical process in a multidimensional state space, reconstructed from the observed time series, using time delay embedding. The Apen statistic is, in essence, the Kolmogorov entropy (Grassberger and Procaccia, 1983). The latter represents the averaged rate of information produced by a dynamical system. The essential difference between these two concepts is that, for calculating the Apen statistic, the embedding dimension m of the reconstructed dynamics and the bin size σ, or a characteristic scale length, are kept constant. Reducing the bias in the Apen statistic due to counting self-matches in the signal patterns, Richman and Moorman (2000) proposed the sample entropy (Sampen) statistic.

Let x_t, $t=1,\ldots,N$ where N is the number of data points, be realizations of a dynamical process μ_x. Next, we assume that the dynamics of the underlying m-dimensional system is reconstructed from the observed time series x_t using time delay embedding

$$x_m(t) = \left(x_t, x_{t-1}, \ldots, x_{t-m+1}\right)^T \quad (1)$$

for all $t=1,\ldots,N-m+1$.

Author's personal copy

Let $\Theta(u)$ denote the Heaviside function, *i.e.* $\Theta(u)=1$ if $u>0$, and $\Theta(u)=0$ if $u<0$, and $\|\cdot\|$ stand for the maximum norm distance between two delay vectors. The function

$$B_i^m(x_m(i),r) = \frac{1}{N-m-1}\sum_{j,j\neq i}\Theta(r-\|x_m(i)-x_m(j)\|) \tag{2}$$

for a given point i with the delay vector $x_m(i)$ reflect the number of points j such that the distance between the vectors $x_m(i)$ and $x_m(j)$ is less than r, excluding self-matches $i=j$. Similar to the $(m+1)$-dimensional representation of x_t, the function

$$A_i^m(x_{m+1}(i),r) = \frac{1}{N-m-1}\sum_{j,j\neq i}\Theta(r-\|x_{m+1}(i)-x_{m+1}(j)\|) \tag{3}$$

for a given delay vector $x_{m+1}(i)$, is proportional to the number of points j such that the distance between the vectors $x_{m+1}(i)$ and $x_{m+1}(j)$ is less than r. Averaging the functions $B_i^m(x_m(i),r)$ and $A_i^{m+1}(x_{m+1}(i),r)$ across all the points $x_m(i)$ and $x_{m+1}(i)$, $i=1,\ldots,N-m$, respectively, we define

$$B^m(r) = \frac{1}{N-m}\sum_i B_i^m(x_m(i),r) \tag{4}$$

and

$$A^m(r) = \frac{1}{N-m}\sum_i A_i^{m+1}(x_{m+1}(i),r) \tag{5}$$

Then, the sample entropy is defined as

$$\mathrm{Sampen}(m,r) = \lim_{N\to\infty} -\ln\frac{A^m(r)}{B^m(r)} \tag{6}$$

which can be estimated as

$$E(m,r) = -\ln\frac{A^m(r)}{B^m(r)} \tag{7}$$

Sampen can be interpreted in terms of the average natural logarithm of conditional probability that two delay vectors, which are close in m-dimensional space (meaning that the distance between them is less than the scale length r), will remain close in $(m+1)$-dimensional space. A greater likelihood of remaining close results in smaller values for the Sampen statistic, indicating less irregularities. Conversely, higher values are associated with the signals having more complexity and less regular patterns in their representations.

In this paper, we will use the statistic designed as inverted complexity, which might be called regularity, namely

$$R = E_{\max} - E \tag{8}$$

where $E_{\max}$ is the maximal sample entropy value for a set of signals under investigation. The $E_{\max}$ value is presumably attributable to some highly irregular dynamics (noise). Higher regularity in the signals, equivalent to lower complexity, produces higher values in statistic (8), and vice versa. Note that the statistic R is limited between 0 and some maximum value $R_{\max}$, presumably associated with the steady-state response phenomenon.

Synchrony: cross-sample entropy

Similar in concept to the Apen statistic, cross approximate entropy was introduced to assess the degree of dissimilarity or asynchrony between two different signals. Later cross-sample entropy (Cross-Sampen) was proposed as a refined version of the cross approximate entropy statistic. Definition of Cross-Sampen is similar to the Sampen measure as defined in (6).

Let $x_m(t)=(x_t,x_{t-1},\ldots,x_{t-m+1})^T$ and $y_m(t)=y_t,y_{t-1},\ldots,y_{t-m+1})^T$ be m-dimensional representations of two dynamical process μ_x and μ_y, respectively. One of these signals might be called template, the other one, target. The function

$$B_i^m(r)\left(\mu_y\|\mu_x\right) = \frac{1}{N-m}\sum_j\Theta(r-\|x_m(i)-y_m(j)\|) \tag{9}$$

for a given point $x_m(i)$ reflects the number of points $y_m(j)$ such that the distance between the vectors $x_m(i)$ and $y_m(j)$ is less than r. Also, the function

$$A_i^m(r)\left(\mu_x\|\mu_y\right) = \frac{1}{N-m}\sum_j\Theta(r-\|y_{m+1}(i)-x_{m+1}(j)\|) \tag{10}$$

for a given delay vector $x_{m+1}(i)$, is proportional to the number of points j such that the distance between the vectors $x_{m+1}(i)$ and $x_{m+1}(j)$ is less than r. Then, averaging across all the points i, the functions $B^m(r)(\mu_y\|\mu_x)$ and $A^m(r)(\mu_x\|\mu_y)$ are defined as

$$B^m(r)\left(\mu_y\|\mu_x\right) = \frac{1}{N-m}\sum_i B_i^m(r)\left(\mu_y\|\mu_x\right) \tag{11}$$

and

$$A^m(r)\left(\mu_x\|\mu_y\right) = \frac{1}{N-m}\sum_i A_i^m(r)\left(\mu_x\|\mu_y\right) \tag{12}$$

Similar to Sampen, Cross-Sampen can be estimated as follows

$$C(m,r) = -\ln\frac{A^m(r)\left(\mu_x\|\mu_y\right)}{B^m(r)\left(\mu_y\|\mu_x\right)} \tag{13}$$

Cross-sample entropy is a measure of nonlinear temporal affiliation between multivariate representations of time course of two signals. Assume that we have two pairs of points randomly taken from two signals at two time points, which are the same for both signals. Cross-sample entropy is related to the probability that the distance between the two points of one signal will be less than some characteristic scale length, given that the distance between the two points of the other signal is also less than that scale length. So, this probability will be low if the dynamics of one signal is not similar to the dynamics of the other signal. From this point of view, the dynamics, for example, of two sine waves are represented by the same circular patterns in a multivariate space, regardless of any phase delay between them. A possible phase delay will just rotate all the points around an axis passing through 0 without any disruption of relative distances between the data points. Thus, it does not affect the probability that two randomly chosen points will remain close (less than a given scale length r), when first we look at one signal and then at the other.

Two highly non-synchronized signals would produce high values of statistic (13), and vice versa (note the minus and the logarithm function in (13)). The asynchrony measure $C(m,r)$ can be transformed into a relative synchrony statistic for a set of signals, subtracting the estimates of $C(m,r)$ from the maximum of the cross-sample entropy values found for all the time series:

$$S = C_{\max} - C \tag{14}$$

A pair of highly synchronized signals from this set of signals would generate higher values of the synchrony statistic S, compared to less synchronized signals from the same set.

Author's personal copy

Data analysis

First, MEG data were down-sampled to a 250 Hz sampling rate, and separated into trials of 5 s duration including 1 s pre-stimulus and 1 s post-stimulus intervals. The stimulus was of 3 s duration. For each MEG sensor and each trial, the baseline correction was achieved by subtracting the mean signal strength across the pre-stimulus interval, and a band pass filter was applied between 16 and 28 Hz. Based on the prior knowledge about the SSSR, we isolated the steady-state MEG data as the time interval from 500 ms after stimulus onset to the end of the stimulus train, [0.5 3.0] s. The first half second was discarded to avoid possible transitory effects.

Source activity was reconstructed with synthetic aperture magnetometry (SAM) (Robinson and Vrba, 1999). The nasion and left/right pre-auricular points were identified on the subjects' anatomical MRI to co-register the MEG data. Isolating the scalp in the MRI generated a realistic head model for source estimation. Based on this head model and the steady-state MEG data, a weighting coefficient set was determined at each node on a $5\times5\times5$ mm grid encompassing the whole brain using a data-driven linearly constrained minimum variance beam-former (Van Veen et al., 1997; Robinson and Rose, 1999). The coefficient sets, in linear combination with the MEG data, estimated the source activity at each grid node to generate whole brain estimates of neuronal activity over time. For more details on the preprocessing procedures and source reconstruction, see Bardouille and Ross (2008). The methods for estimating complexity and asynchrony were applied to the reconstructed steady-state source activity time series.

Further, the steady-state time series for each voxel were normalized to have 0 mean and unit variance. The embedding dimension m for computing the sample and cross-sample entropy statistics was set to 5. The rationale for this is based on empirical observations: the sample entropy decreased with m, and reached its floor values for about $m=5{,}6$. To identify brain areas with consistently regular dynamics, the complexity was computed according to (7) on a voxel-by-voxel basis, for all the single trials, with subsequent averaging across trials. Thus, one value was associated with one source location. Next we transformed the complexity map (E) into a regularity map (R) by subtracting the E statistic for individual source locations from the maximal value $E_{\max}$ of the given subject's complexity map, according to (8).

To create asynchrony volumetric maps, we chose a source from a peak location in the primary somatosensory area (SI) contralateral to stimuli. In calculating the cross-sample entropy statistic, the dynamics at area SI were treated as the template, whereas the target was the rest of the brain, on a source-by-source basis. Similar to the complexity maps, asynchrony (C) maps for each subject were converted to synchrony (S) maps, subtracting the cross-sample entropy values for individual source locations from their absolute maximum.

The volumetric maps of complexity/regularity and synchrony/asynchrony were co-registered with the corresponding anatomical MRI images by identifying the head localization coil locations in the MRI image. For each subject, the anatomical MRI image was transformed into Talairach space, and we applied the same transformation to the complexity/regularity maps. Further, the Talairach-transformed anatomical MRI images were averaged across subjects to give an anatomical reference. In addition, the regularity and synchrony maps for individual subjects were averaged across subjects. The means were tested for stability across group, based on permutation tests by bootstrap resampling of subjects (Efron and Tibshirani, 1993). The bootstrap ratio, which is defined as the ratio of the mean value to the bootstrap standard deviation, is approximately equivalent to a z-score and can be used as a measure of stability across subjects. The absolute bootstrap ratio values higher than 3.5 correspond roughly to a 99% confidence interval. We used AFNI software (Cox, 1996) to visualize the volumetric data, with the anatomical MRI data as the underlay images, and the maps of regularity or synchrony serving as the overlay images.

Results

Simulations

This section describes "proof-of-principle" simulations emphasizing the method based on complexity analysis described above. The objective is to demonstrate the performance of the sample and cross-sample entropy statistics in the presence of two active dipoles coded as SI and SII. We chose one anatomical MRI data set from the pool of subjects. Specified in Talaraich coordinate system, two source locations were $x=-40$ m [L], $y=-20$ mm [P], and $z=84$ mm [S] for SI, and $x=-50$ m [L], $y=0$ mm [P], and $z=50$ mm [S] for SII. For all 84 trials, the dynamics of both sources represented 23 Hz sine waves of 3 s duration, sampled at the rate of 250 samples per second. The sources were of 20 nAm peak amplitude. There was no amplitude or phase jitter across trials for source SI. In contrast to SI, SII was phase-randomized by jittering the phase by ±5.5 ms. Forward solution of the induced magnetic field in the sensor space was performed with a single sphere model in the default position of $x=0$, $y=0$, $z=5$ cm. Gaussian noise with peak to peak level of 150 fT filtered to a bandwidth of 1 to 50 Hz was added to the sensor signals.

Dynamics of simulated MEG source activity was reconstructed with SAM (Robinson and Vrba, 1999), similar to the analysis performed on real data. The linear constrained minimum variance beam-former (Van Veen et al., 1997) was applied to estimate the corresponding weighting coefficients defining the source dynamics as a linear combination of all MEG sensor signals. Complexity analysis as described in Complexity: sample entropy was thereafter performed based on reconstructed synthetic source dynamics for individual trials with subsequent averaging of the estimated sample entropy values across trials. The complexity map was inverted to regularity map by subtracting the complexity values from their maximum.

The regularity values were between 0 and 0.115. Fig. 1 illustrates a color map of the trial-averaged regularity statistic R thresholded at the level of 0.069, which is 60% of the observed maximum. The color bar (g) is included to indicate the magnitude range of the regularity statistic. The volumetric regularity maps shown on axial (a, b), coronal (c, d), and sagittal (e, f) views are localized in with good correspondence to the locations of the modeled sources SI and SII.

Synchrony volumetric map was calculated seeding a source from the location SI. Keeping the SI dynamics as the template whereas the target was the rest of the brain, cross-sample entropy was computed, on a voxel-by-voxel basis for all single trials with subsequent averaging across trials. Then, the asynchrony map was inverted into the synchrony map, with high values representing an increase in synchrony between SI and a given source, as shown in Fig. 2. We identified two peaks in the synchrony field. First, SI was found to be synchronized with itself. In addition, SII was identified as having a high degree of affiliation with SI. Note that the link was not designed to be phase-locked as in generating source SII we jittered its phase. Nevertheless, there was a strong coupling between SI and SII in terms of the similarity of multidimensional signal patterns.

Physiological data

We applied the data analysis, as described in Discussion, by computing volumetric sample entropy maps for individual subjects. Averaging the individual regularity maps across subjects, we were able to clearly identify three peaks. Specifically, the peaks were found in contralateral area SI, and bilaterally in the posterior parietal cortex (PPC). The neural dynamics in these sources were characterized by lower values of sample entropy statistic E, or inversely, higher values of regularity statistic R. In other words, the neural dynamics of the somatosensory steady state at the area SI contralateral to the stimuli and bilateral PPC were less irregular in comparison to all other source locations.

Author's personal copy

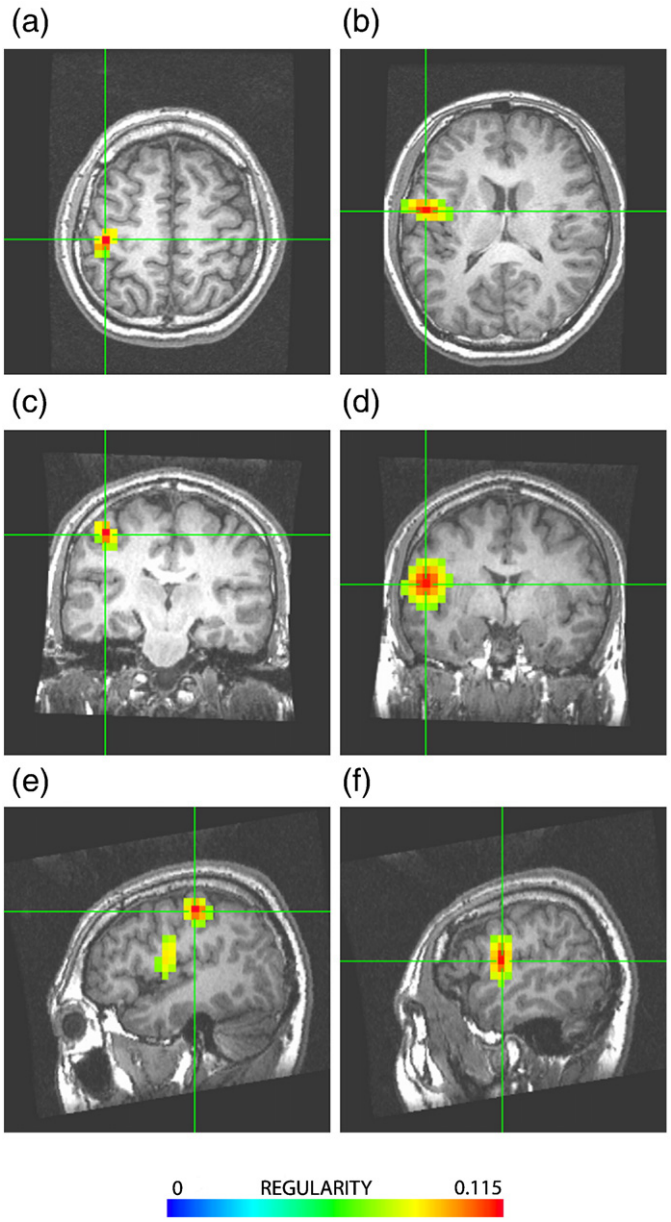

Fig. 1. Axial, coronal, and sagittal views of volumetric map of the regularity statistic, based on synthetic source dynamics data. The white crosses are centered on the peaks in the regularity field. The estimates of the regularity statistic were between 0 and 0.115, with high values associated with a decrease in signal complexity. The map is thresholded at the level of 60% of the maximal value. The peaks are localized with good correspondence to the locations of the modeled sources: SI (a, c, e) and SII (b, d, f).

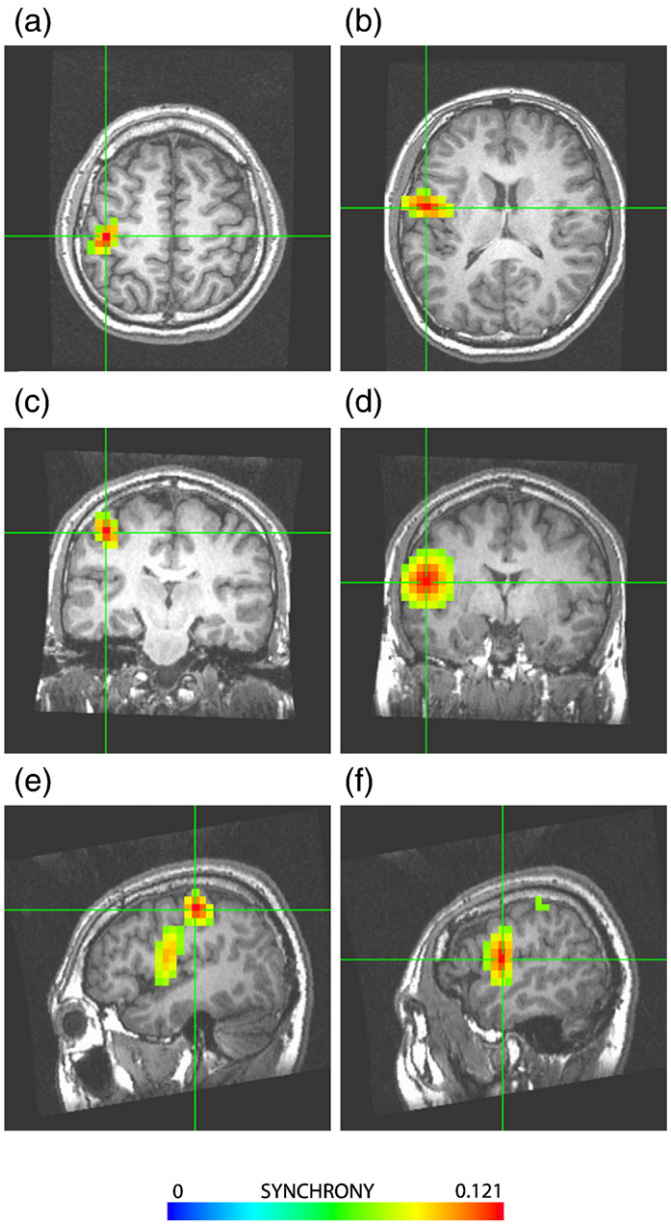

Fig. 2. Axial, coronal, and sagittal views of the volumetric map of the synchrony statistic. It is based on the same synthetic data as used to construct the regularity map shown in Fig. 1. The synchrony map was calculated seeding source SI. The synchrony statistics were between 0 and 0.121, with high values associated with more synchrony between SI and the rest of the brain. The map is thresholded at the level of 60% of the maximal value. Two peaks were identified: SI (a, c, e) as synchronized with itself and SII (b, d, f). Note that, by construction, the dynamics of SI and SII are not phase-locked.

The values of the regularity statistic R averaged across subjects were between 0 and 0.026. Fig. 2 shows the volumetric subject-averaged map of regularity (inverted complexity) for three locations: (a, d, g) contralateral SI; (b, e, h) left PPC; (c, f, i) right PPC. The regularity map thresholded at the level of 60% of its maximum is superimposed on the subject-averaged anatomical MRI. The group average complexity map R is displayed in coronal, axial, and sagittal planes. The color bar included at the bottom of Fig. 2 indicates the magnitude distribution of the regularity statistic R averaged across subjects. Higher values coded in red colors are associated with a decrease in complexity of the steady-state response in given source locations.

Similar to the complexity analysis, bilateral activation of the PPC was observed on the synchrony maps based on seeding an activated source from the contralateral SI. Specifically, averaging the individual synchrony maps (S) across subjects, we clearly identified the same peaks as those observed visualizing the complexity field. The values of the synchrony statistic R averaged across subjects were between 0 and 0.022. Fig. 3 shows the volumetric subject-averaged map of synchronized interactions for the same three locations: contralateral SI, and left and right PPC, as illustrated in Fig. 2. The synchrony map is thresholded at the level of 60% of its maximum, and superimposed on the subject-averaged anatomical MRI. The map shows three main peaks, contralaterally in the area SI and bilaterally in PPC. Specified in Talairach coordinate system, the peak location associated with source SI was found to be around $x=-44$ m [L], $y=-31$ mm [P], and $z=47$ mm [S], whereas the coordinates of PPC sources were around $x=\pm 43$ mm [L/R], $y=-46$ mm [P], and $z=34$ mm [S].

Author's personal copy

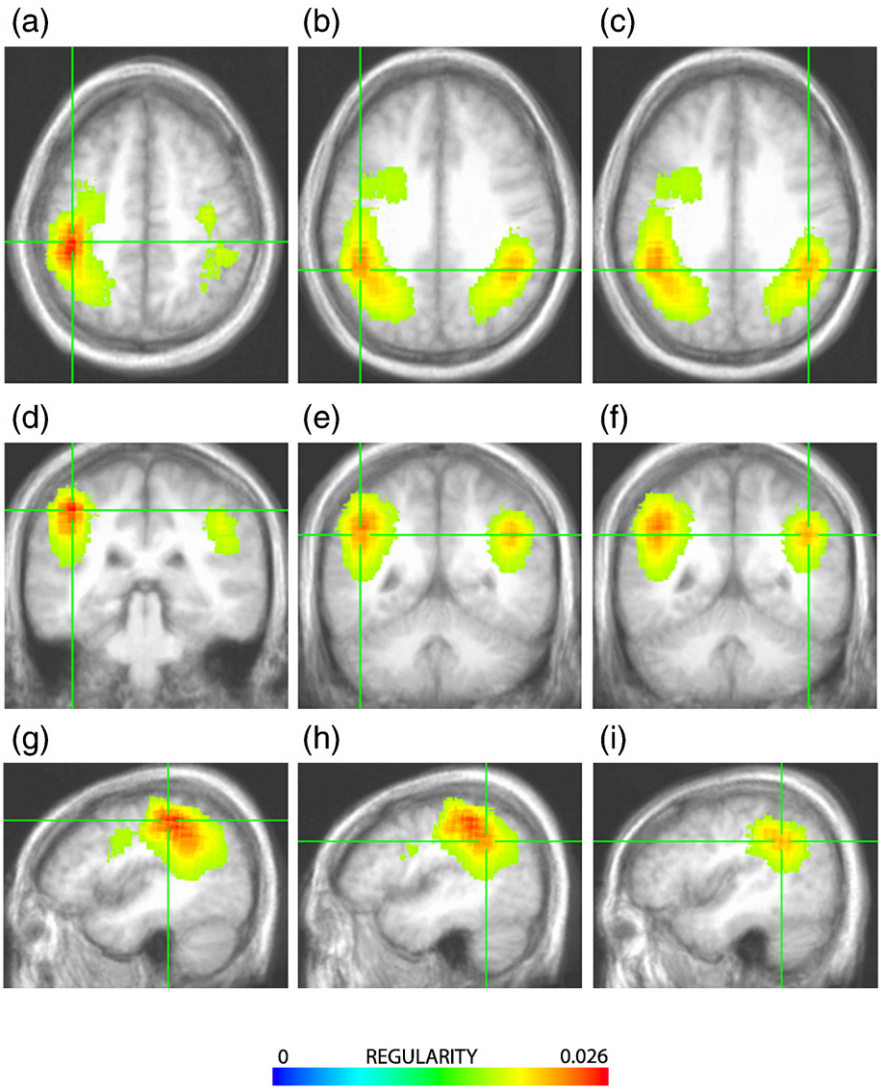

Fig. 3. Axial, coronal, and sagittal views of volumetric regularity (inverted complexity) map of the somatosensory steady-state response. The complexity map averaged across subjects is superimposed on the subject-averaged anatomical MRI. The map is shown for peak locations in the regularity map: (left column) primary somatosensory area (SI) contralateral to the tactile stimuli; (middle column) left posterior parietal cortex (PPC); (right column) right PPC. The map is thresholded at the level of 60% of the maximum regularity value of 0.026. The white crosses are centered on the local peaks. Higher values coded in red colors are associated with a decrease in complexity of the steady-state response at a given location in comparison to the rest of the brain.

We tested the sample and cross-sample statistics for significance. The means were tested for stability across group, based on permutation tests by bootstrap resampling of subjects, as described in Discussion. The bootstrap ratio values, which are defined as the ratio of the mean values to the bootstrap standard deviation, were computed both for the sample and cross-sample entropy maps. The complexity and synchrony statistics for the regions SI and PPC, averaged across subjects, were found significant with the bootstrap ratio values greater than 10, which corresponds to more than 99% confidence.

With regards to the synchrony map, the trivial result is that the sources in the area SI are well synchronized with themselves in two different representations: m- and $(m+1)$-dimensional state spaces. The second result is related to an increase in synchrony between areas SI and PPC in comparison to the synchrony between SI and all other sources. The complexity and asynchrony results seem to support one another. It is encouraging to identify the interaction network that is in good accordance with the activation map revealed by a complexity statistic. The synchrony map provides extra information in the sense that the dynamics of the two areas are driven by the same effect (Fig. 4).

Discussion

Somatosensory cortical activity is encoded topographically according to the body surface. The discovery of this somatotopic organization of the somatosensory cortex SI in humans can be traced back to Penfield and Boldrey (1937). In addition to SI, other brain areas were found to be sensitive to tactile stimuli, including the PPC regions, the secondary somatosensory cortex (SII), supplementary motor area (SMA), and primary motor cortex (MI) (Forss et al., 2001; Hyvarinen, 1982; Nangini et al., 2006; Strick and Preston, 1982). PPC is densely connected to the regions of somatosensory cortex. Since the early electrophysiological studies in monkeys, PPC has been considered as a higher order associated somatosensory region (Hyvarinen, 1982). Furthermore, a number of studies reported results in relation to the hypothesis about somatotopic organization of PPC able to code the locations of external objects or body parts (Andersen et al., 1997; Duhamel et al., 1992). In particular, Hoshiyama et al. (1997) investigated PPC to determine its functional role as a somatosensory associated area using MEG measurements. Based on a multidipole model of brain electric sources, they identified activities in SI contralateral to stimulation and bilateral PPC as a reaction to stimulating median and posterior tibial nerves.

Author's personal copy

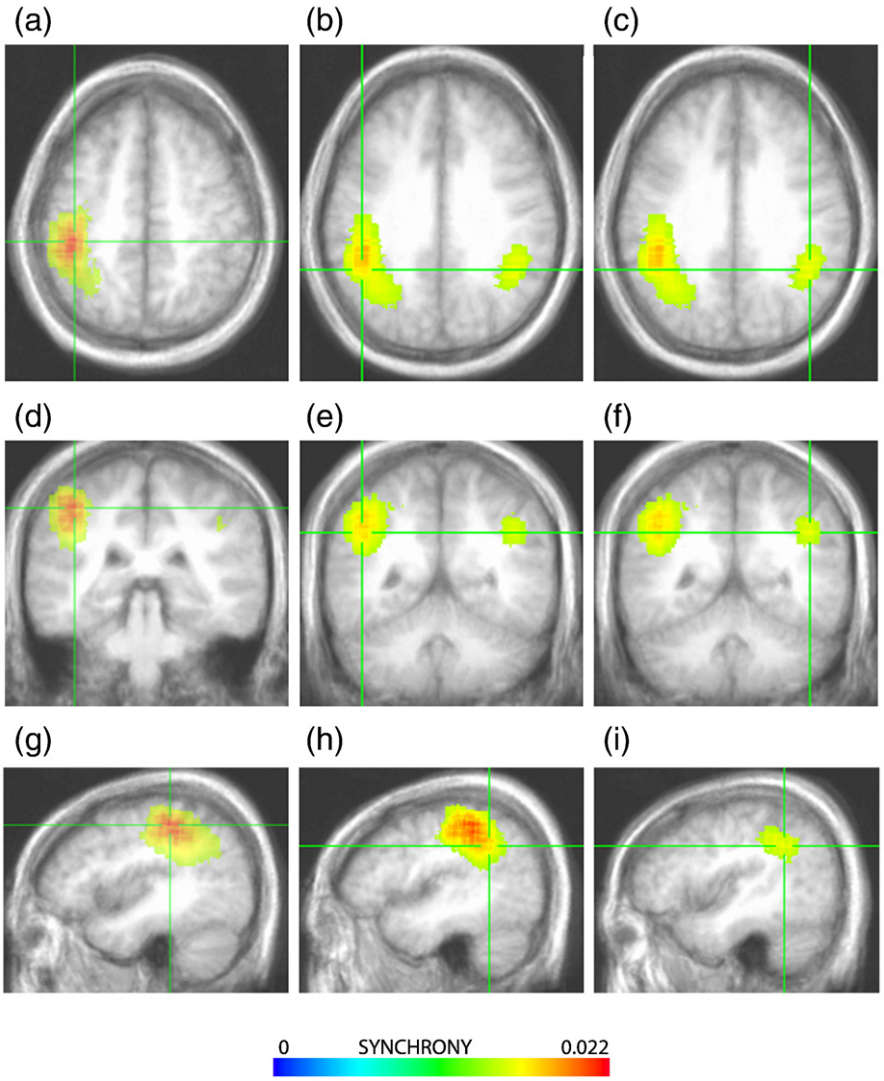

Fig. 4. Axial, coronal, and sagittal views of volumetric synchrony map of the somatosensory steady-state response for a source in the primary somatosensory area (SI) contralateral to stimuli. The synchrony map averaged across subjects is superimposed on the subject-averaged anatomical MRI. Similar to the complexity map illustrated in Fig. 1, the synchrony map is shown for its peak locations: (left column) primary somatosensory area (SI) contralateral to the tactile stimuli; (middle column) left posterior parietal cortex (PPC); (right column) right PPC. The map is thresholded at the level of 60% of the maximum synchrony value of 0.014. The white crosses are centered on the local peaks. Higher values of the synchrony statistic coded in red colors are associated with a decrease in asynchrony between neural dynamics in the contralateral area SI and a given source relative to the rest of the brain.

This study presented a completely data-driven approach to characterize the neural components of the somatosensory steady-state response within the framework of signal complexity. Specifically, we analyzed the steady-state response as a reaction to high-rate repetitive stimuli, applying mechanical pressure pulses to the right finger. The sample and cross-sample entropy analysis was performed in the source space based on the dynamics of neural sources reconstructed using a SAM beam-former technique without any assumption for the underlying dipole model. For each source location, the complexity and synchrony statistics were computed for all the single trials, and then averaged across trials. Reflecting the relative degree of regularity of source dynamics, complexity maps were constructed using the sample entropy statistic. Seeding an activated source from area SI, synchrony maps were computed based on the cross-sample entropy. To identify consistent common features robustly expressed across subjects we generated the group-averaged complexity and synchrony maps. It is pleasing that for synchrony analysis, we do not use an *a priori* defined set of regions of interest. Instead, the patterns of interactions between activated regions emerged automatically on the noisy background.

The subject-averaged volumetric maps of complexity revealed patterns in the area SI contralateral to the stimuli, and bilaterally in the PPC regions. These areas were characterized by decreased complexity or, in other words, increased regularity of their dynamics. Visualizing the subject-averaged synchrony map constructed with respect to the template from the area SI, we were able to identify the same topographic organization as that based on the complexity analysis. Specifically, oscillatory dynamics of the sources in SI had a higher degree of affiliation with that of the sources in PPC, compared to the rest of the brain. Such results are partly supported by the cross-sample entropy analysis: the synchronized network is based on the same topographic structure of sample entropy map. Hierarchically, finding the synchronized behavior of the SI and PPC regions seems to be a stronger conclusion than detecting their separate activation, adding new information on their simultaneous activation.

We did not see any reduced complexity into the secondary somatosensory area SII. It was shown that neuromagnetic activity in SII during median nerve stimulation was characterized by a sustained DC shift rather than oscillatory activity (Forss et al., 2001). The methods used in the manuscript are based on the dynamic oscillations at the stimulus

Author's personal copy

frequency (the data were band pass filtered in the beta range), and there is no reason to believe that they would be sensitive to a sustained source.

We should note that the map of peaks is definitely dependent on a threshold. In this situation, caution should be exercised as it is practically unfeasible to find the best criterion that is able to distinguish correctly what looks like a real peak from what might be just a noisy fluctuation in the tomographic map. In setting the right threshold, visual analysis is just as reliable as advanced statistical criteria, if not the most trusted. In an attempt to find an optimal threshold, we looked at the tomographic maps and thresholded them at different levels. Our visual inspection revealed that in the range of threshold of about 60%–65% of its maximum, there are no other peaks except those that were reported in the manuscript. At the level of 55%–60%, we were able to observe other local maxima, but we would not describe them as distinctive peaks, as they merged with the main peaks with further lowering of the threshold by a few percents. We believe that setting the threshold at around 60%–80% of its maximum qualitatively shows the structure of the tomographic maps of sample and cross-sample entropy.

Finally, it is worth discussing the feasibility of the complexity approach to the intertrial coherence (ITC), which is widely used in the literature at least since the book by Mardia (1972). Using ITC, Bardouille and Ross (2008) analyzed the whole-head neuromagnetic source dynamics, measuring the amount of phase synchrony inherent in a given signal across repeated presentations of stimuli. Although they observed increased phase-locked activity in PPC for individual subjects, there was no consistency in the group results. At the same time, high phase-locking factor was a consistent feature of the area SI.

In contrast to ITC, statistics such as sample or cross-sample entropy based on multidimensional representations of original signals identified PPC and SI, both consistently expressed across a group of subjects. Comparing the results of ITC and complexity analysis, one could characterize the somatosensory steady-state response in SI as both phase-locked to stimuli and highly regular (with low complexity) in terms of its amplitude dynamics. In contrast, posterior parietal regions seem not to be activated synchronously, at least not for a given signal-to-noise ratio, in the sense of phase-locking, with vibrotactile stimulation of an index finger, although their dynamics are represented by regular multidimensional patterns that are preserved from trial to trial. As we can see, these patterns are well coordinated with those in SI, not necessarily being phase-locked. This allows one to extend our description of functional integration between brain regions working together to perform a specific task. Phase locking alone may not be adequate enough to properly describe interactions between activated areas. Temporal coordination between events in terms of similar multidimensional signal patterns may complement the phenomena of synchronization between brain regions.

Acknowledgments

We wish to thank Maria Tassopoulos for her assistance in preparing this manuscript.

References

Absolo, D., Hornero, R., Espino, P., Poza, J., Snchez, C.I., de la Rosa, R., 2005. Analysis of regularity in the EEG background activity of Alzheimer's disease patients with approximate entropy. Clin. Neurophysiol. 1160 (8), 1826–1834.

Andersen, R.A., Snyder, L.H., Bradley, D.C., Xing, J., 1997. Multimodal representation of space in the posterior parietal cortex and its use in planning movements. Annu. Rev. Neurosci. 20, 303–330.

Bardouille, T., Ross, B., 2008. MEG imaging of sensorimotor areas using intertrial coherence in vibrotactile steady-state responses. Neuroimage 420 (1), 323–331.

Bruhn, J., Rpcke, H., Rehberg, B., Bouillon, T., Hoeft, A., 2000. Electroencephalogram approximate entropy correctly classifies the occurrence of burst suppression pattern as increasing anesthetic drug effect. Anesthesiology 930 (4), 981–985.

Costa, M., Goldberger, A.L., Peng, C.K., 2002. Multiscale entropy analysis of physiologic time series. Phys. Rev. Lett. 89, 062102.

Cox, R.W., 1996. AFNI: software for analysis and visualization of functional magnetic resonance neuroimages. Comput. Biomed. Res. 29 (3), 162–173.

Deisboeck, T.S., Kresh, J.Y. (Eds.), 2006. Complex systems in science in biomedicine. Springer.

Duhamel, J.R., Colby, C.L., Goldberg, M.E., 1992. The updating of the representation of visual space in parietal cortex by intended eye movements. Science 2550 (5040), 90–92.

Efron, B., Tibshirani, R.J., 1993. An Introduction to the Bootstrap. Chapman and Hall.

Forss, N., Narici, L., Hari, R., 2001. Sustained activation of the human SII cortices by stimulus trains. Neuroimage 130 (3), 497–501.

Gmez, C., Hornero, R., Absolo, D., Fernndez, A., Escudero, J., 2009. Analysis of MEG background activity in Alzheimer's disease using nonlinear methods and ANFIS. Ann. Biomed. Eng. 370 (3), 586–594.

Grassberger, P., Procaccia, I., 1983. Estimation of the Kolmogorov entropy from a chaotic signal. Phys. Rev. A 28, 2591–2593.

Hornero, R., Absolo, D., Escudero, J., Gmez, C., 2009. Nonlinear analysis of electroencephalogram and magnetoencephalogram recordings in patients with Alzheimer's disease. Philos. Trans. A Math. Phys. Eng. Sci. 367 (1887), 317–336.

Hoshiyama, M., Kakigi, R., Koyama, S., Watanabe, S., Shimojo, M., 1997. Activity in posterior parietal cortex following somatosensory stimulation in man: magnetoencephalographic study using spatio-temporal source analysis. Brain Topogr. 10 (1), 23–30.

Hyvarinen, J., 1982. Posterior parietal lobe of the primate brain. Physiol. Rev. 62 (3), 1060–1129.

Jirsa, V.K., McIntosh, A.R. (Eds.), 2007. Handbook of Brain Connectivity. Springer-Verlag, Berlin Heidelberg.

Mardia, K.V., 1972. Statistics of Directional Data. Academic Press.

McIntosh, A.R., Kovacevic, N., Itier, R.J., 2008. Increased brain signal variability accompanies lower behavioral variability in development. PLoS Comput. Biol. 4 (7), e1000106.

Nangini, C., Ross, B., Tam, F., Graham, S.J., 2006. Magnetoencephalographic study of vibrotactile evoked transient and steady-state responses in human somatosensory cortex. Neuroimage 33 (1), 252–262.

Nunez, P.L., Shrinivasan, R., 2005. Electric Fields in the Brain: The Neurophysics of EEG. University Press, Oxford.

Penfield, W., Boldrey, E., 1937. Somatic motor and sensory representation in the cerebral cortex of man as studied by electrical stimulation. Brain 60, 389–443.

Pincus, S.M., 1991. Approximate entropy as a measure of system complexity. Proc. Natl. Acad. Sci. U. S. A. 88, 2297–2301.

Pincus, S., 1995. Approximate entropy (ApEn) as a complexity measure. Chaos 5 (1), 110–117.

Radhakrishnan, N., Gangadhar, B.N., 1998. Estimating regularity in epileptic seizure time-series data. A complexity-measure approach. IEEE Eng. Med. Biol. Mag. 17 (3), 89–94.

Richman, J.S., Moorman, J.R., 2000. Physiological time-series analysis using approximate entropy and sample entropy. Am. J. Physiol Heart Circ. Physiol. 278 (6), H2039–H2049.

Robinson, S.E., Rose, D.F., 1999. Biomagnetism: Clinical Aspects, Chapter Current Source Estimation by Spatially Filtered MEG. Excerpta Medica, Amsterdam, pp. 761–765.

Robinson, S.E., Vrba, J., 1999. Recent Advances in Biomagnetism, Chapter Functional Neuroimaging by Synthetic Aperture Magnetometry. Tohoku University Press, Sendai, pp. 302–305.

Snyder, A.Z., 1992. Steady-state vibration evoked potentials: descriptions of technique and characterization of responses. Electroencephalogr. Clin. Neurophysiol. 840 (3), 257–268.

Stam, C.J., 2005. Nonlinear dynamical analysis of EEG and MEG: review of an emerging field. Clin. Neurophysiol. 1160 (10), 2266–2301.

Stapells, D.R., Makeig, S., Galambos, R., 1987. Auditory steady-state responses: threshold prediction using phase coherence. Electroencephalogr. Clin. Neurophysiol. 67 (3), 260–270.

Strick, P.L., Preston, J.B., 1982. Two representations of the hand in area 4 of a primate. II. somatosensory input organization. J. Neurophysiol. 48 (1), 150–159.

Van Veen, B.D., van Drongelen, W., Yuchtman, M., Suzuki, A., 1997. Localization of brain electrical activity via linearly constrained minimum variance spatial filtering. IEEE Trans. Biomed. Eng. 44 (9), 867–880.

Womelsdorf, T., Schoffelen, J.M., Oostenveld, R., Singer, W., Desimone, R., Engel, A.K., Fries, P., 2007. Modulation of neuronal interactions through neuronal synchronization. Science 316 (5831), 1609–1612.